Journal of
Materials Chemistry C

RSCPublishing

PAPER

View Article Online
View Journal

Cite this: DOI: 10.1039/c3tc30592a

Observation of the room temperature phosphorescence of Bodipy in visible light-harvesting Ru(II) polyimine complexes and application as triplet photosensitizers for triplet–triplet-annihilation upconversion and photocatalytic oxidation†

Wanhua Wu, Jifu Sun, Xiaoneng Cui and Jianzhang Zhao*

Received 30th March 2013
Accepted 21st May 2013

DOI: 10.1039/c3tc30592a

www.rsc.org/MaterialsC

Two Ru(II) polyimine complexes containing a boron-dipyrromethene (Bodipy) chromophore were prepared. The two complexes are different in the linker which connects the Bodipy part and the Ru(II) coordination centre. The Bodipy core and the Ru(II) centre are in π-conjugation in **Ru-1**, whereas in **Ru-2** the Bodipy part is linked in a non-conjugated way to the Ru(II) centre. Ru(bpy)$_3$[PF$_6$]$_2$ (**Ru-3**) was used as a reference complex. Both **Ru-1** and **Ru-2** show strong absorption in the visible region ($\varepsilon = 65\,200$ M^{-1} cm^{-1} at 528 nm for **Ru-1** and $\varepsilon = 76\,700$ M^{-1} cm^{-1} at 499 nm for **Ru-2**). The fluorescence of the Bodipy ligands was almost completely quenched in **Ru-1** and **Ru-2**. **Ru-1** shows room temperature phosphorescence of the Bodipy chromophore, as well as the residual fluorescence of the Bodipy ligand. **Ru-2** shows only the residual fluorescence of the Bodipy ligand. A long-lived Bodipy-localized triplet excited state was observed for both **Ru-1** and **Ru-2** upon visible light excitation (τ_T is up to 279.7 μs, the longest T$_1$ state lifetime observed for the Bodipy moiety in the transition metal complex). Application of the complexes in triplet–triplet-annihilation upconversion and singlet oxygen ($^1O_2$)-mediated photooxidation proved that **Ru-1** is more efficient (*e.g.* singlet oxygen quantum yield $\Phi_\Delta = 0.93$) as a triplet photosensitizer than **Ru-2** ($\Phi_\Delta = 0.64$). Therefore, direct connection of the π-core of the Bodipy chromophore to the coordination centre, *i.e.* by establishing π-conjugation between the visible light-harvesting chromophore and the metal coordination centre is essential to enhance the effective visible light-harvesting of the Ru(II) complexes.

Introduction

Recently Ru(II) polyimine complexes have attracted much attention owing to the applications in photocatalysis such as photoredox reactions,[1–3] photoinduced H$_2$ production from water,[4] photocatalytic cleavage of DNA,[5,6] luminescent molecular probes and bioimaging,[7–12] photovoltaics,[13–16] and triplet–triplet-annihilation upconversion.[17] However, the conventional Ru(II) polyimine complexes, such as Ru(bpy)$_3$[PF$_6$]$_2$ (bpy = 2,2′-bispyridine), show weak absorption in the visible region ($\varepsilon < 20\,000$ M^{-1} cm^{-1} in the region beyond 400 nm), and the absorption maxima are usually at 450 nm. Furthermore, the triplet excited state lifetimes of the typical Ru(II) complexes are usually shorter than 5 μs.[2,8,16,18,19] These photophysical features are detrimental to the applications of Ru(II) polyimine complexes as triplet photosensitizers in the new applications, such as photocatalysis.

In order to address these challenges, Ru(II) complexes with long-lived triplet excited states were prepared, based on the mechanisms of either establishment of triplet state equilibrium[2,20–27] or population of the ligand-centred IL state[19,28–30] or by optimization of the coordination geometry of the *N^N* ligands.[31] However, it is still a challenge to enhance the effective absorption of Ru(II) complexes in the visible region.[1–19]

Previously the coumarin unit was used as a visible light-harvesting ligand for the Ru(II) complex, but the absorption band is in the UV region.[32,33] Dipyrrin was used as a ligand for Ru(II) complexes, but the generation of the triplet excited state and the application of the resulted visible light-absorbing complexes were not reported.[34] Concerning this aspect, Bodipy is a versatile chromophore which shows intense absorption in the visible range.[35–52] Bodipy was also attached to the Ru(II) coordination framework but very often the phosphorescence of the Ru(II) coordination center and the Bodipy fluorophore was quenched.[25,46] Furthermore, the triplet excited states of

---

State Key Laboratory of Fine Chemical, School of Chemical Engineering, Dalian University of Technology, Dalian, 116024, P.R. China. E-mail: zhaojzh@dlut.edu.cn; Web: http://finechem.dlut.edu.cn/photochem; Fax: +86 411-8498-6236

† Electronic supplementary information (ESI) available: Molecular structure characterization data, UV/Vis absorption and emission spectra and TTA upconversion details. See DOI: 10.1039/c3tc30592a

the complexes were not investigated in detail. Recently we attached Bodipy moieties to the Ir(III) coordination center and long-lived triplet excited states were observed.[17c] Based on the pioneering studies from other groups, we postulate that the intramolecular energy transfer can be enhanced with selection of a suitable linker between the visible light-harvesting antenna and the coordination center.[46,53,54] Concerted energy levels for the light-harvesting ligands and the Ru(II) coordination center are also important. To date the application of the long-lived triplet excited state of Ru(II) complexes has rarely been reported.[20,21,28,53] The visible light-absorbing Bodipy-containing Ru(II) complexes were not studied for any applications.

In order to address these challenges, herein we prepared two Ru(II) polyimine complexes, in which the Bodipy units were either linked in a way of π-conjugation to the coordination center *via* a C≡C bond (**Ru-1**), or tethered on the *N^N* coordination framework (**Ru-2**, Scheme 1). Ru(bpy)$_3$[PF$_6$] was used as a reference complex. The structure of **Ru-2** is similar to the conventional Ru(II)–Bodipy complexes,[25,46] but the structural profile of **Ru-1** is unprecedented for the Bodipy-containing Ru(II) complexes.[21] The photophysical properties of the complexes were studied by steady state and time-resolved absorption and photoluminescence spectroscopy. Both **Ru-1** and **Ru-2** show strong absorption of visible light and long-lived triplet excited states. The complexes were used

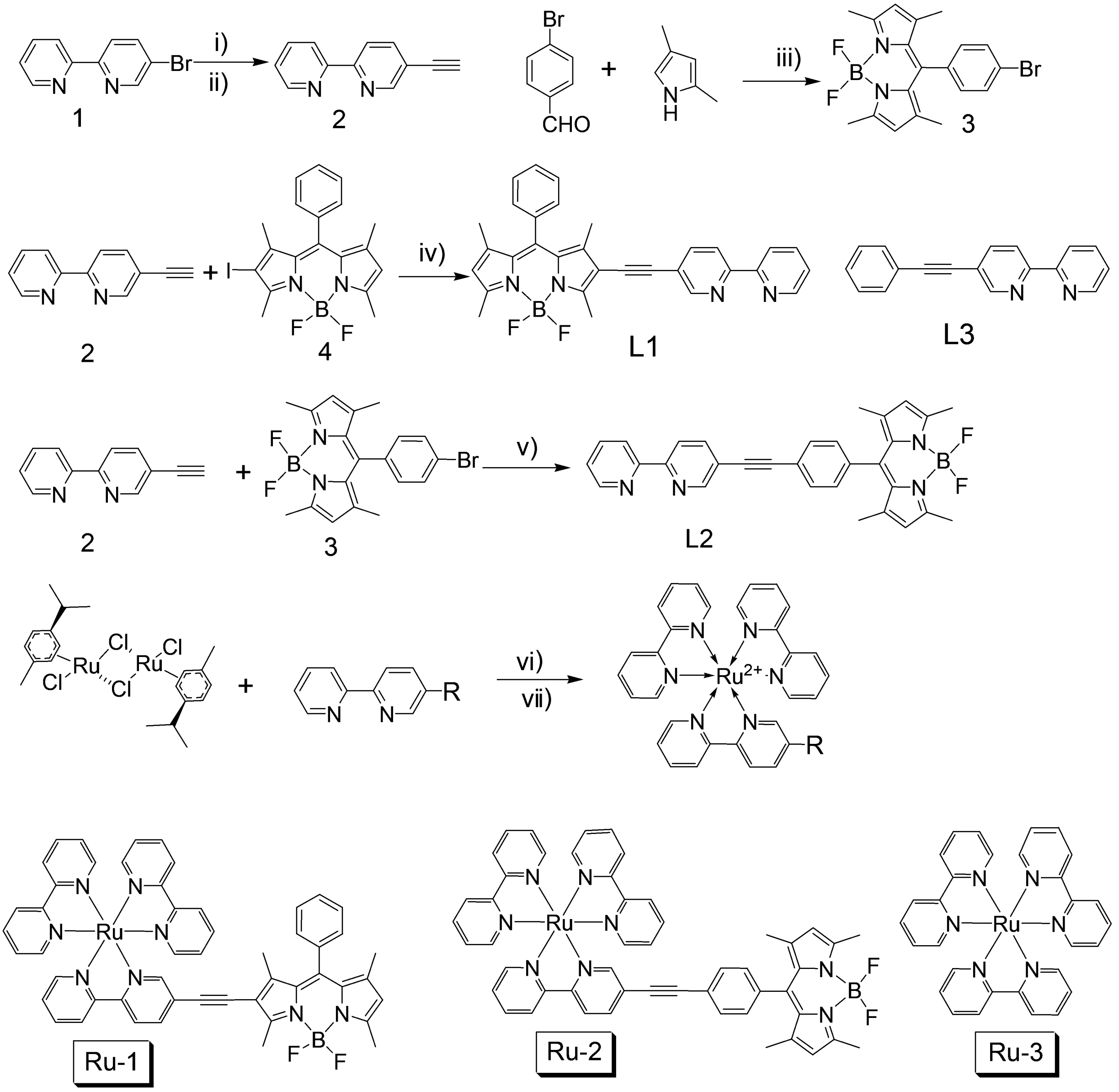

Scheme 1 Synthesis of the ligands **L1** and **L2** and the complexes **Ru-1** and **Ru-2**, and the structure of model compound **L3** and complex **Ru-3** were also shown. The complexes are positively charged and the anions PF$_6^-$ are omitted for clarity. *Reagents and conditions*: (i) trimethylsilylacetylene, Pd(PPh$_3$)$_2$Cl$_2$, PPh$_3$, CuI, NEt$_3$, reflux, 8 h; (ii) Bu$_4$NF, THF, r.t. (iii) dry CH$_2$Cl$_2$, CF$_3$COOH, DDQ, BF$_3$–Et$_2$O, NEt$_3$; (iv) Pd(PPh$_3$)$_2$Cl$_2$, PPh$_3$, CuI, THF/NEt$_3$, reflux, 8 h; (v) Pd(PPh$_3$)$_4$, CuI, THF/NEt$_3$, reflux, 14 h; (vi) ethanol, r.t., 3 h; (vii) 2,2′-bipyridine, ethanol–H$_2$O, reflux, 22 h.

as triplet photosensitizers in triplet–triplet annihilation (TTA) upconversion and singlet oxygen ($^1O_2$)-mediated photooxidation of organic substrates. The results demonstrated that the efficiency of **Ru-1** as a triplet photosensitizer in these applications is much higher than that of **Ru-2**. These molecular structural design rationales, the photophysical studies and the applications may be useful for future development of visible light-harvesting Ru(II) complexes and for the applications of these complexes in photocatalysis and TTA upconversion.

Experimental section

General analytical measurements

NMR spectra were recorded on a Bruker 400 MHz spectrometer ($CDCl_3$ or acetone-d_6 as solvents, TMS as a standard, $\delta = 0.00$ ppm). High resolution mass spectra (HRMS) were recorded on a LC/Q-TOF MS system (UK). Luminescence spectra were recorded on a RF-5301 PC or a CRT 970 spectrofluorometer. Fluorescence lifetimes were measured with an OB920 luminescence lifetime spectrometer (Edinburgh, UK). Absorption spectra were recorded on an Agilent 8453A UV/Vis spectrophotometer. The nanosecond time-resolved transient difference absorption spectra were measured by Edinburgh analytical instruments (LP920, Edinburgh Instruments, Livingston, UK) and recorded on a Tektronix TDS 3012B oscilloscope. The synthesis of compound **4** was reported elsewhere.[55] For detailed synthetic procedures of compounds **1**, **2** and **3**, NMR spectra, MS spectra and spectroscopic experiments, please refer to the ESI.†

Ligand L1

Under Ar atmosphere, 2-iodo-1,3,5,7-tetramethyl-8-phenyl-4,4-difluoro-4-bora-3a-azonia-4a-aza-*s*-indacene (**4**) (70.0 mg, 0.16 mmol) and 5-ethynyl-2,2′-bipyridine (**2**) (33.6 mg, 0.19 mmol) were added to the mixed solvent of THF–triethylamine (5 : 2, v/v, 7 mL). The flask was vacuumed and back-filled with Ar for three times, and then $Pd(PPh_3)_2Cl_2$ (5.6 mg, 0.008 mmol, 5 mol %), PPh_3 (0.016 mmol, 4.2 mg, 10 mol%) and CuI (0.016 mmol, 3.2 mg, 10 mol%) were added under Ar atmosphere. The mixture was refluxed for 8 h under Ar atmosphere. After completion of the reaction, the mixture was cooled to RT and the solvents were evaporated under reduced pressure. The crude product was purified with column chromatography (silica gel, CH_2Cl_2–$CH_3OH = 300 : 1$, v/v) to give the red solid, 35.0 mg, 43.8%. ^{1}H NMR (400 MHz, $CDCl_3$) $\delta = 8.72$ (s, 1H), 8.44 (s, 1H), 7.87 (d, 2H, $J = 5.2$ Hz), 7.53–7.52 (m, 4H), 7.31–7.29 (m, 3H), 6.06 (s, 1H), 2.73 (s, 3H), 2.60 (s, 3H), 1.52 (s, 3H), 1.41 (s, 3H); ^{13}C NMR (100 MHz, $CDCl_3$) $\delta = 158.6$, 156.4, 155.2, 151.4, 149.0, 145.4, 142.9, 142.4, 139.1, 137.6, 134.7, 130.4, 129.5, 128.0, 124.2, 122.6, 121.7, 120.7, 114.5, 92.9, 87.1, 15.0, 14.8, 13.8, 13.4; MALDI-HRMS: calcd ($[C_{31}H_{25}BF_2N_4]^+$), $m/z = 502.2140$, found, $m/z = 502.2149$.

Ligand L2

Under Ar atmosphere, 1,3,5,7-tetramethyl-8-(4-bromophenyl)-4,4-difluoroboradiazaindacene (**3**) (80.0 mg, 0.2 mmol) and 5-ethynyl-2,2′-bipyridine (**2**) (35.8 mg, 0.2 mmol) were added to the mixed solvents of THF–triethylamine (5 mL/2 mL). Then $Pd(PPh_3)_4$ (0.02 mmol, 23.1 mg, 10 mol%) and CuI (0.04 mmol, 8.0 mg, 20 mol%) were added under Ar atmosphere. The mixture was refluxed and stirred for 14 h under argon. After completion of the reaction, the mixture was cooled to RT, the solvents were evaporated under reduced pressure. The crude product was purified by column chromatography (silica gel, CH_2Cl_2–$CH_3OH = 300 : 1$, v/v) to give 30.0 mg red solid (30.0%). ^{1}H NMR (400 MHz, $CDCl_3$) $\delta = 8.85$ (s, 1H), 8.71 (s, 1H), 8.45 (s, 2H), 7.98–7.96 (d, 1H, $J = 4.5$ Hz), 7.86 (s, 1H), 7.72 (d, 2H, $J = 5.2$ Hz), 7.34 (m, 3H), 2.56 (s, 6H), 1.44 (s, 6H); ^{13}C NMR (100 MHz, $CDCl_3$) $\delta = 156.0$, 155.4, 151.9, 149.4, 143.1, 140.7, 139.7, 137.3, 135.7, 132.5, 131.3, 128.6, 124.3, 123.6, 121.6, 120.7, 120.1, 92.9, 87.9, 14.8. ESI-HRMS: calcd ($[C_{31}H_{25}BF_2N_4 + H]^+$) $m/z = 503.2219$; found, $m/z = 503.2223$.

General method for the preparation of the Ru(II) complexes

$RuCl_2$(cymene) (0.5 eq.) and ligands (1.0 eq.) were suspended in ethanol (5.0 mL). The mixture was stirred at r.t. under N_2 atmosphere for *ca.* 2 h until the solution become clear. Then a solution of 2,2′-bipyridine (2.0 eq.) in water (10 mL) was added and the mixture was refluxed for 22 h. After cooling, the solvent was evaporated under reduced pressure. The crude product was then subjected to column chromatography (silica gel eluted with acetonitrile : water : saturated aqueous $NaNO_3 = 100 : 9 : 1$, v/v) and treated with a saturated aqueous solution of NH_4PF_6. Red precipitate was collected with filtration, the solid was washed with water and dried in a vacuum.

Complex Ru-1

Following the general procedure outlined above, ligand **L1** (20.0 mg, 0.04 mmol) was added, and the complex **Ru-1** was isolated in 38.4% yield (18.5 mg). ^{1}H NMR (400 MHz, acetone-d_6): 8.83–8.78 (m, 6H), 8.24–8.20 (m, 7H), 8.11–8.04 (m, 4H), 7.89 (s, 1H), 7.65–7.58 (m, 8H), 7.49–7.43 (m, 2H), 6.32 (s, 1H), 2.57 (s, 3H), 2.46 (s, 3H), 1.45 (s, 5H), 1.38 (s, 3H); ^{13}C NMR (100 MHz, acetone-d_6) $\delta = 160.97$, 157.86, 157.70, 156.07, 152.64, 152.38, 147.23, 143.49, 142.10, 139.14, 138.67, 134.63, 134.20, 133.82, 130.08, 129.52, 128.40, 125.24, 124.98, 124.59, 123.98, 91.55, 88.64, 14.57, 14.42, 13.05, 12.75. ESI-HRMS: $[(M\text{-}2PF_6)^{2+}/2]$ calcd, $m/z = 458.1274$; found, $m/z = 458.1292$.

Complex Ru-2

Following the general procedure outlined above, ligand **L2** (15 mg, 0.03 mmol) was added, and the complex **Ru-2** was isolated in 35.4% yield (12.8 mg). ^{1}H NMR (400 MHz, acetone) $\delta = 8.89$–8.82 (m, 5H), 8.37 (d, 1H, $J = 8.0$ Hz), 8.24–8.22 (m, 7H), 8.11–8.06 (m, 3H), 8.03 (d, 1H, $J = 5.2$ Hz), 7.70 (d, 2H, $J = 7.8$ Hz), 7.60–7.59 (m, 5H), 7.52 (d, 2H, $J = 7.9$ Hz), 6.13 (s, 2H), 2.50 (s, 6H), 1.41 (s, 6H); ^{13}C NMR (101 MHz, acetone-d_6) $\delta = 157.46$, 155.88, 152.26, 152.00, 142.99, 140.97, 140.32, 138.33, 132.62, 131.06, 128.23, 127.97, 124.61, 121.67, 95.61, 80.98, 13.97. ESI-HRMS: $[(M\text{-}2PF_6)^{2+}/2]$ calcd, $m/z = 458.1274$; found, $m/z = 458.1292$.

Calculations

The optimization of the ground state geometry and the spin density surface of the Ru(II) complexes were calculated based on the optimized triplet state geometry at the B3LYP/6-31 G/LANL2DZ level with Gaussian 09W.[56] The UV/Vis absorption, and the S_0/T_1 energy gaps of the complexes were calculated with the time-dependent DFT (TDDFT). MeCN was used as a solvent in the calculations (PCM model).

TTA upconversion

A diode pumped solid state laser was used in the TTA upconversions. The upconversion quantum yields (Φ_{UC}) were determined with the prompt fluorescence of 2,6′-diiodo-Bodipy (Φ = 9.3% in toluene) as the standard. The upconversion quantum yields were calculated with eqn (1), where Φ_{UC} stands for the upconversion quantum yields, A, I and η represent the absorbance, integrated photoluminescence intensity and the refractive index of the solvent, sam represents the sample, and std represents the standard (eqn (1)). The equation is multiplied by factor 2 in order to make the maximum quantum yield to be unity.[17a]

$$\Phi_{UC} = 2\Phi_{std}\left(\frac{1-10^{-A_{std}}}{1-10^{-A_{sam}}}\right)\left(\frac{I_{sam}}{I_{std}}\right)\left(\frac{\eta_{sam}}{\eta_{std}}\right)^2 \tag{1}$$

The TTET efficiency was studied by Stern–Volmer quenching constants. The concentration of the photosensitizers was fixed at 1.0×10^{-5} M. The lifetimes of the photosensitizers were measured by LP920 with increasing perylene or DPA concentration in the solution.

Photooxidation

10 mL CH_2Cl_2–MeOH (9/1, v/v) solution containing DHN (2.0×10^{-4} M) and a photosensitizer (2.0×10^{-5} M) was placed in a round-bottom flask and was irradiated by a 35 W xenon lamp through a 0.72 M $NaNO_2$ solution to cut off the light with wavelength shorter than 385 nm. At intervals of 2–5 min, 2 mL of the mixture was sampled for the UV-Vis absorption measurement and was put back immediately after recording the absorption spectra, and UV/Vis absorption spectra were recorded on the Agilent 8453 UV/Vis spectrophotometer. The power density was tuned to 13 mW cm^{-2} and was measured with a solar power meter. The DHN consumption was monitored by a decrease in the absorption at 301 nm, the concentration of DHN was calculated by using its molar absorption coefficient (ε = 7664 M^{-1} cm^{-1}) at 301 nm. The juglone production was monitored by an increase in the absorption at 427 nm, the concentration of juglone was calculated by using its molar extinction coefficient (ε = 3811 M^{-1} cm^{-1}), and the yield of juglone was obtained by dividing the concentration of juglone with the initial concentration of DHN.

Singlet oxygen ($^1O_2$) quantum yields (Φ_Δ)

Φ_Δ values of the triplet photosensitizers were calculated according to a modified literature method.[57] The light source of a fluorometer was used as the monochromatic light source for irradiation. The irradiation wavelength for the samples and the reference was the same. Quantum yields for singlet oxygen generation in CH_2Cl_2 were determined by monitoring the photooxidation of 1,3-diphenylisobenzofuran (DPBF) sensitized by the Ru(II) complexes. The absorbance of DPBF was adjusted around 1.0 at 414 nm in air saturated CH_2Cl_2, and absorbance of the sensitizers was adjusted to 0.2–0.3 at the irradiation wavelength. The photo-oxidation of DPBF was monitored at the interval of 10 s. The quantum yields of singlet oxygen generation (Φ_Δ) were calculated by a relative method using TPP (Φ_Δ = 0.62) and Rose Bengal (Φ_Δ = 0.80 in MeOH) as the reference. The following equation was used,

$$\Phi_\Delta^{sam} = \Phi_\Delta^{std}\frac{m^{sam}F^{std}}{m^{std}F^{sam}} \tag{2}$$

where superscripts 'sam' and 'std' designate Ru complexes and the standards, respectively, Φ_Δ is the quantum yield of singlet oxygen, m is the slope of a plot of difference in change in absorbance of DPBF (at 420 nm) with the irradiation time and F is the absorption correction factor, which is given by $F = 1 - 10^{-A}$.

Results and discussion

Molecular design and synthesis of the Ru(II)–Bodipy complexes

In the typical Ru(II) polyimine complexes, such as $Ru(bpy)_3^{2+}$ (bpy = 2,2-bispyridine), π-conjugation between the Ru(II) coordination center and the N^N ligand can be established by the ligand-to-metal bonding and the metal-to-ligand π bonding, also called "π-backbonding". For **Ru-1**, the π-core of the Bodipy chromophore is directly linked to the bpy ligand *via* a π-conjugation linker of the C≡C bond. Thus we anticipate red-shifted absorption for **Ru-1** *vs.* the ligand **L1**. For **Ru-2**, however, the linkage is at the meso-phenyl moiety of Bodipy. The π-conjugation framework of bpy in **Ru-2** is not extended significantly. Therefore we anticipated similar absorption for **Ru-2** compared to that for **L2**. The different linkers between the Bodipy chromophore and the bpy ligand may impose a significant effect on the ISC of Ru(II) complexes. Previously Bodipy was attached to the coordination center of the Ru(II) complexes, but all those complexes are with the Bodipy chromophore isolated from the coordination center.[46] The preparation of the complexes is based on the iodination of the Bodipy and Pd(0)-catalyzed Sonogashira coupling reactions. All the compounds were obtained in satisfactory yields.

UV-Vis absorption of the Ru(II) complexes

The UV-Vis absorption spectra of Bodipy ligands and complexes were studied (Fig. 1). **L1** gives absorption at 527 nm, which is red-shifted compared to the ligand **L2** (λ_{abs} = 499 nm). The difference in the absorption of **L1** and **L2** can be attributed to the larger π-conjugation framework in **L1** than **L2**. We noted that the absorption spectrum of **L2** is the sum of the absorption of Bodipy and phenylethynyl bpy (**L3**), indicating the lack of π-conjugation between bpy and Bodipy parts in **L2**.

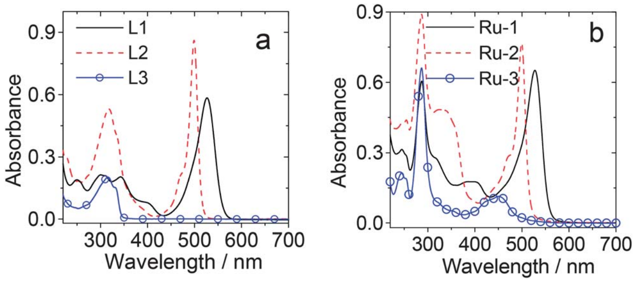

Fig. 1 UV-Vis absorption spectra of the (a) ligands and (b) complexes **Ru-1–Ru-3**. $c = 1.0 \times 10^{-5}$ M in MeCN, 20 °C.

Compared to the reference complex **Ru-3**, both **Ru-1** and **Ru-2** show much stronger absorption in the red-shifted region (at 528 nm and 499 nm, respectively, Fig. 1b). Notably the molar absorption coefficients (ε) are up to 76 700 M^{-1} cm^{-1}. To the best of our knowledge, Ru(II) complexes with such strong visible light absorption are rarely reported.[2,22,25,46] The absorption of **Ru-1** and **Ru-2** in the visible range is similar to the ligands **L1** and **L2**, and is comparable to the reported dipyrrin Ru(II) complexes that show strong absorption in the visible region.[16,34]

Photoluminescence of the Ru(II) complexes

The luminescence of the ligands and complexes was studied (Fig. 2). **L1** and **L2** give strong emission at 563 nm and 512 nm, respectively. In comparison, the Ru(II) complexes give much weaker emission, and the fluorescence emission of the ligands was substantially quenched in the complexes. This quenching effect may be due to the energy transfer, intersystem crossing (ISC), or electron transfer process.[25]

The photoluminescence of the complexes was investigated (Fig. 2c and d). **Ru-1** gives emission at 741 nm in deaerated solution. The emission band was substantially quenched in aerated solution, indicates the triplet state origin of this emissive band (phosphorescence). For **Ru-2**, however, the phosphorescence band centered at 650 nm was observed, and the residual fluorescence of the Bodipy unit is more significant than that in **Ru-1**. The reference complex **Ru-3** gave the normal ^{3}MLCT phosphorescence at 608 nm and the emission band can be quenched by O_2 (see ESI† for detail). Based on the emission wavelength of **Ru-1**, the emission band was attributed to the RT phosphorescence of Bodipy.[25,46,58] For **Ru-2**, the phosphorescence emission band at 648 nm can be attributed to the normal ^{3}MLCT emission of the polyimine Ru(II) complexes.

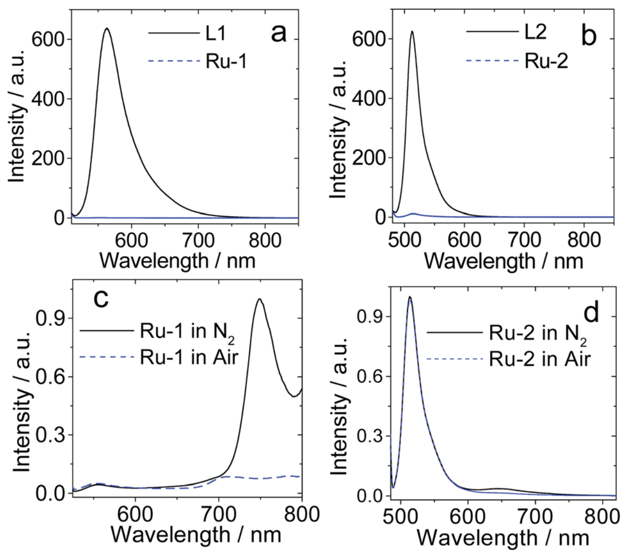

Fig. 2 Emission spectra of (a) **Ru-1** and the ligand **L1** ($\lambda_{ex} = 520$ nm) in N_2, (b) **Ru-2** and **L2** ($\lambda_{ex} = 480$ nm) in N_2; emission spectra of the complexes (c) **Ru-1** ($\lambda_{ex} = 520$ nm) and (d) **Ru-2** ($\lambda_{ex} = 480$ nm) under different atmospheres of N_2 and air (MeCN, 1.0×10^{-5} M; 20 °C).

To the best of our knowledge, this is the first time that the RT phosphorescence of Bodipy was observed with Ru(II) complexes.[25,46,59] The Bodipy–Ru(II) complexes reported previously share a similar molecular structural profile with **Ru-2**, as a result the heavy atom effect is non-efficient and the RT phosphorescence of the Bodipy part cannot be observed.[25,59] We propose that the heavy atom effect in **Ru-1** is more significant than that in **Ru-2**, therefore the ISC is more efficient in **Ru-1**. It should be noted that the emission quantum yields and the triplet excited state lifetime of the Ru(II) coordination center would not be altered given the T_1 state energy level of the organic chromophore is higher than the ^{3}MLCT state.[3]

Comparison of the luminescence excitation spectra and the UV-Vis absorption spectra

In order to study the intramolecular energy transfer of the complexes,[33,42,47] the luminescence excitation spectra of the complexes were recorded and were compared with the UV-Vis absorption spectra (Fig. 3). For the reference complex **Ru-3** (Fig. 3c), the excitation spectrum is superimposable to the UV-Vis absorption (Fig. 3c), indicating that the ^{3}MLCT emission is directly resulted from the $S_0 \rightarrow {}^1$MLCT excitation.

For **Ru-1**, the emission wavelength was set at 740 nm, *i.e.* the ^{3}IL state emission localized on the Bodipy part. We found that the absorption of the Bodipy part at 528 nm is effective to produce the near IR emission at 740 nm. For **Ru-2**, with setting the emission wavelength at 650 nm, only the MLCT absorption band is effective to produce the emission. The absorption of the Bodipy part at 500 nm is un-effective to produce the emission at 650 nm. For the emission at 540 nm (emission of the Bodipy part), the absorption at 500 nm is effective. These results indicate that the ^{3}MLCT state cannot be accessed with excitation into the absorption band of Bodipy in **Ru-2**. That is, the strong absorption of **Ru-2** is not effective to produce the ^{3}MLCT state, which is in stark contrast to **Ru-1** (Fig. 3a). These results indicated that for **Ru-2**, the ^{1}Bodipy* → ^{1}MLCT process is non-efficient.

Emission spectra of the complexes at 77 K

The photoluminescence spectra of the complexes at 77 K were measured (Fig. 4). Compared to the emission spectra at RT, the fluorescence emission of **Ru-1** at 550 nm in the RT spectrum disappeared at 77 K, and only an emission band at 741 nm was observed, which is slightly blue shifted *vs.* the emission at RT (Fig. 4a). This small thermally induced Stokes shift (ΔE_S) is a

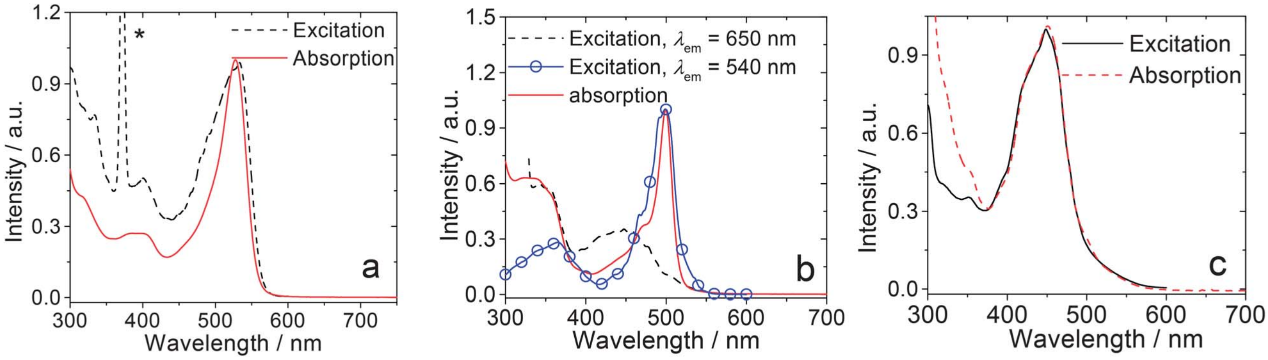

Fig. 3 Comparison of the normalized UV-Vis absorption and the excitation spectra of the complexes (a) **Ru-1** (the peak denoted with asterisk is due to the second order transmission of the monochromator), (b) **Ru-2** and (c) **Ru-3**. The excitation spectra of **Ru-1** were recorded with $\lambda_{em} = 740$ nm, for **Ru-2**, $\lambda_{em} = 650$ nm and 540 nm, for **Ru-3**, $\lambda_{em} = 607$ nm. $c = 1.0 \times 10^{-5}$ M in MeCN, 20 °C.

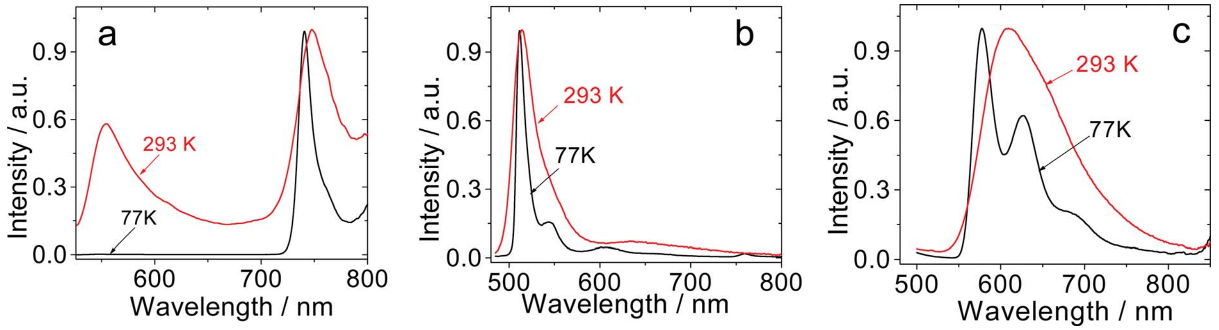

Fig. 4 Emission spectra of (a) **Ru-1** ($\lambda_{ex} = 520$ nm), (b) **Ru-2** ($\lambda_{ex} = 480$ nm) and (c) **Ru-3** ($\lambda_{ex} = 450$ nm) in ethanol–methanol (4 : 1, v/v) glass at 77 K and in solution at RT.

clear indication of the emissive ^{3}IL state for **Ru-1**. For **Ru-2**, however, no Bodipy phosphorescence emission in the near-IR region was observed (Fig. 4b), which is in agreement with the reported Bodipy–Ru(II) complexes that share a similar structural profile with **Ru-2**.[46] For the reference complex **Ru-3** (Fig. 4c), the emission spectrum become more structured and blue-shifted compared to that at RT. The large thermally induced Stokes shift of **Ru-3** indicated the ^{3}MLCT feature of the emissive triplet excited state of **Ru-3**, which is in full agreement with the known photophysics of **Ru-3**.[21]

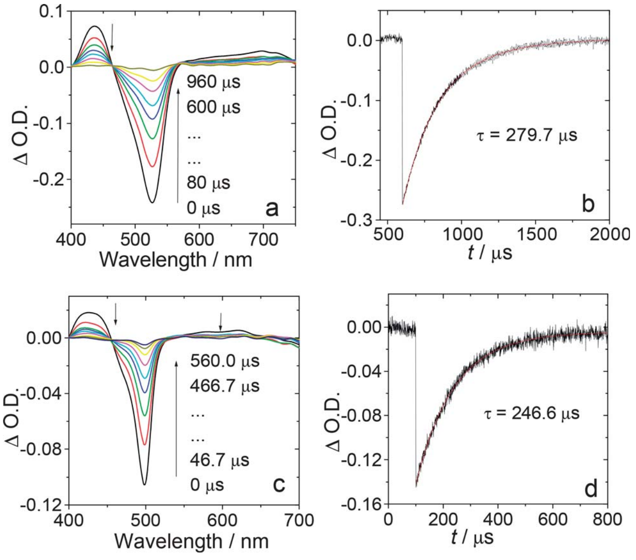

Fig. 5 Nanosecond time-resolved transient difference absorption spectra of (a) **Ru-1** and (c) **Ru-2** after pulsed excitation ($\lambda_{ex} = 532$ nm); decay traces of (b) **Ru-1** at 530 nm and (d) **Ru-2** at 500 nm. $c = 1.0 \times 10^{-5}$ M in MeCN 20 °C.

Nanosecond time-resolved transient difference absorption spectra

In order to study the triplet excited state of the complexes, the nanosecond time-resolved transient difference absorption spectra of the complexes were studied (Fig. 5). Upon 532 nm photoexcitation, significant bleaching at 530 nm was observed for **Ru-1** (Fig. 5a), which is due to the depletion of the ground state of the Bodipy ligand. Therefore the triplet excited state of **Ru-1** is localized on the Bodipy part. The lifetime of the triplet excited state was determined as 279.7 μs (Fig. 5b). To the best of our knowledge, this is the longest triplet state lifetime observed for the Bodipy chromophore.[25,46] Previously the lifetime of the Bodipy triplet state was observed in the range of 8–30 μs.[25,46] Interestingly, similar transients were observed for **Ru-2** (Fig. 5c), with slightly blue-shifted bleaching bands. Thus the triplet excited state of **Ru-2** is also localized on the Bodipy part, not the Ru(II) coordination center. We propose that this result is due to the lower energy level of the Bodipy ^{3}IL state compared to the ^{3}MLCT state.[25,46] The triplet state lifetime of **Ru-2** was

Table 1 Photophysical parameters of the Ru(II) complexes and the ligands[a]

			Emission properties				
	λ_{abs}	ε^b	λ_{em}/nm	$\lambda_{em}{}^c$/nm	$\Phi_L{}^d$ (%)	$\tau_F{}^e$/ns	$\tau_T{}^f$
Ru-1	528	6.52	748	741	—[h]	—[h]	279.7 μs/33.9[g] ms
Ru-2	499	7.67	513	510	1.0	0.14	246.6 μs/4.4[g] μs
Ru-3	451	1.14	608	578	9.6	—[h]	0.8 μs/5.4[g] μs
L1	527	5.85	563	—[h]	33.6	3.5	—[h]
L2	499	8.64	512	—[h]	43.9	1.9	—[h]

[a] Result of complexes in MeCN solution (1.0×10^{-5} mol dm^{-3}), 293 K. [b] Molar absorption coefficient at the absorption maxima, ε 10^4 M^{-1} cm^{-1}. [c] Result in ethanol–methanol (4 : 1, v/v) glass at 77 K. [d] With BODIPY ($\Phi = 0.72$ in THF) as the standard. [e] Fluorescence lifetime. [f] Triplet lifetimes measured by nanosecond time-resolved transient absorptions. [g] Luminescence lifetime at 77 K. [h] Not determined.

determined as 246.6 μs. In comparison, the triplet state lifetime of the model complex **Ru-3** was determined as 0.8 μs (^{3}MLCT state, see ESI† for details). These results proved that the lowest-lying triplet states of **Ru-1** and **Ru-2** are drastically different from that of **Ru-3**. Since the energy transfer from ^{1}Bodipy → ^{1}MLCT is inhibited in **Ru-2** due to the unmatched energy levels of the singlet excited states, the heavy atom effect in **Ru-2** is weak, the generation of the ^{3}IL state in **Ru-2** may be due to the charge re-combination process.[25] It should be noted that Ru(II) complexes with a triplet excited state lifetime up to 200 μs were not reported.[2,21,22,29] The photophysical parameters of the Ru(II) complexes and the ligands are summarized in Table 1.

Previously Ru(II) complexes with thermally equilibrated ^{3}MLCT and ^{3}IL states were prepared, but the lifetimes were much shorter.[21] For example, a triplet state lifetime of 42 μs was observed for a pyrenyl ethynyl polyimine Ru(II) complex.[18] The pyrene unit was attached to the *N^N* ligand of the Ru(II) complex by a C–C bond (similar to the profile of **Ru-2**) and a long-lived pyrene localized triplet state was observed (148 ± 8 μs).[24] Bodipy was attached to the terpyridine ligand of Ru(II) complexes, but the Bodipy-localized ^{3}IL state is shorter-lived (τ_T = 8–30 μs).[25] Naphthalimide was used for preparation of Ru(II) complexes that show the ^{3}IL/^{3}MLCT state equilibrium and a lifetime of up to 115 μs was observed,[27] but the molar absorption coefficient of the complex in the 400–500 nm region is only 20 000 M^{-1} cm^{-1}. Recently we prepared coumarin-containing Ru(II) complexes that show the ligand-localized triplet excited state, but the T_1 lifetime is much shorter (less than 5 μs).[54] Aryl-borane-containing Ru(II) complexes were also reported and the phosphorescence lifetime is 12 μs.[10,60] Thienyl–dipyrrin Ru(II) complexes were prepared, the visible light absorption of these complexes are strong,[16,34] but the triplet excited states were not investigated. Recently we prepared cyclometalated Ir(III) complexes with Bodipy ligands, but the triplet excited state lifetimes (23.7 μs and 87.2 μs) are much shorter than **Ru-1** and **Ru-2**.[17c]

DFT calculations

Recently it was shown that density functional theory is useful in studying the luminescence properties of transition metal complexes.[61] In order to study the photophysical properties of the complexes **Ru-1** and **Ru-2**, which contain the Bodipy units, DFT calculations were carried out.

Firstly the ground state geometry of the complexes was optimized. For **Ru-1**, the Bodipy chromophore takes a coplanar orientation toward the bpy ligand of the Ru(II) coordination center. As a result, full π-conjugation is expected for the Bodipy π-core and the Ru(II) coordination center. For **Ru-2**, however, the Bodipy π-core takes a perpendicular geometry toward the bpy coordination ligand. Therefore, there is no full π-conjugation between the Bodipy chromophore and the bpy coordination ligand. This different π-conjugation profile will affect the UV/Vis absorption of the complexes.

The UV/Vis absorption of complexes **Ru-1** and **Ru-2** was studied with the time-dependent DFT (TDDFT). The calculated absorption wavelength of **Ru-1** is 499 nm, which is very close to the experimental results (λ_{abs} = 528 nm, Fig. 1b and Table 1). Molecular orbitals of HOMO → LUMO are involved in this $S_0 \rightarrow S_1$ transition. These molecular orbitals are localized on Bodipy as well as the bpy moieties (Fig. 6a). Therefore there is efficient π-conjugation between the Bodipy chromophore and the bpy coordination ligand. The UV/Vis absorption of **Ru-1** was also calculated without any solvents (in vacuum). The calculated $S_0 \rightarrow S_1$ transition is with an absorption wavelength of 854 nm (see ESI† for detail).

The energy gap of the S_0/T_1 states was calculated as 1.57 eV (792 nm), which is very close to the experimental results of 1.66 eV (748 nm, Fig. 4). Since the major components of the $T_1 \rightarrow S_0$ state is LUMO → HOMO, the T_1 state can be identified as the ^{3}IL state, which is localized on Bodipy (Fig. 6a, for the detail of the electronic transitions, please refer to the ESI†). This result is in agreement with the transient difference absorption spectroscopy.

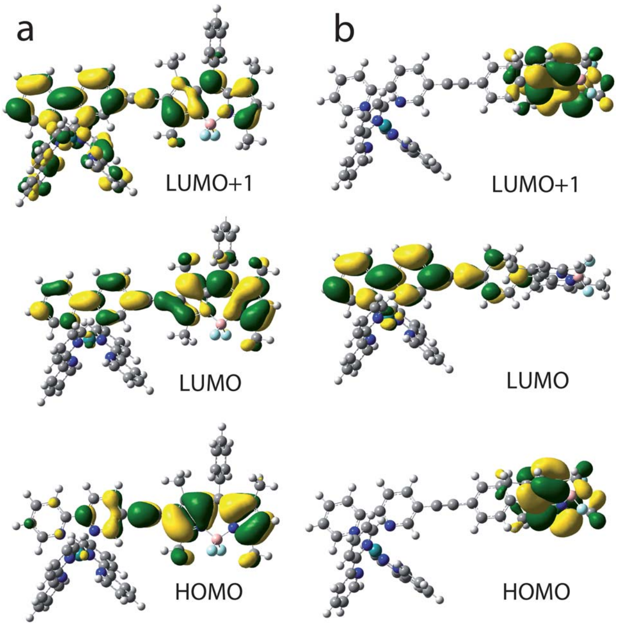

Fig. 6 Frontier molecular orbitals of (a) **Ru-1** and (b) **Ru-2**. Based on the optimized ground state geometry (S_0 state). CH_3CN was used as a solvent. Calculation was performed at the B3LYP/6-31G(d)/LanL2DZ level with Gaussian 09W.

The UV-Vis absorption of **Ru-2** was also calculated with the TDDFT method. Different from **Ru-1**, the LUMO of **Ru-2** is only distributed on the bpy ligand, the electron density map of the orbital is completely isolated from the π-conjugation core of Bodipy (Fig. 6b). The HOMO of **Ru-2** is localized on the π-core of the Bodipy chromophore, which is not spread to bpy (Fig. 6b). Therefore, $S_0 \rightarrow S_1$ transition is a full charge transfer transition, which is often a quantum mechanically forbidden process. This postulation was supported by the oscillator strength ($f = 0.00$) of the calculated $S_0 \rightarrow S_1$ transition. We identified that $S_0 \rightarrow S_8$ transition ($\lambda_{\text{abs}} = 427$ nm, $S_0 \rightarrow S_8$) may be responsible for the main absorption band of **Ru-2** in the visible region (499 nm, Fig. 1b and Table 1). HOMO → LUMO+1 are involved in the transition. LUMO+1 is localized on the Bodipy unit (Fig. 6b). Therefore, the S_8 state can be identified as the ^{1}IL state. It should be pointed out that there is significant deviation for the calculated absorption wavelength (427 nm) from the experimental absorption value of 499 nm (Fig. 1b). However, it was known that very often the unsubstituted Bodipy chromophore cannot be well described by the DFT calculations.

The energy gap of the S_0/T_1 states was calculated as 1.52 eV (816 nm), which is close to the value of **Ru-1** (1.66 eV, 748 nm). HOMO → LUMO+1 are major components of the T_1 state. Therefore, the T_1 state can be described as the ^{3}IL state, which is localized on the Bodipy unit. This postulation is corroborated by the nanosecond time-resolved transient difference absorption spectroscopy of the complexes.

In order to study the localization of the triplet excited states of the complexes from a point of view of theoretical chemistry, the spin density surfaces of the complexes were computed with the DFT method (Fig. 7). This method has not been used for Bodipy-containing Ru(II) complexes.[46] For both **Ru-1** and **Ru-2**, the spin density surfaces are localized on the Bodipy part. The bpy ligands and the Ru(II) centre did not contribute to the spin density surface of the complexes. These results are in full agreement with the transient absorption spectra and the TDDFT calculations. Therefore the lowest lying triplet excited states of **Ru-1** and **Ru-2** are localized on the Bodipy part. For **Ru-3**, however, the spin density surface is localized on the Ru(II) coordination centre and the bpy ligands, which is in agreement with the MLCT feature of the triplet excited state of **Ru-3**.

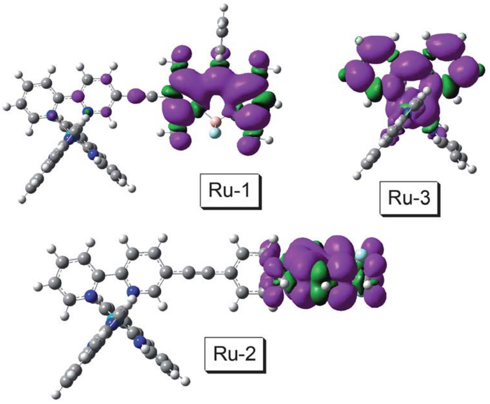

Fig. 7 Isosurfaces of spin density of **Ru-1**, **Ru-2** and **Ru-3** at the optimized triplet state geometries. MeCN was used as a solvent in the calculations (PCM model). Calculation was performed at the B3LYP/6-31G(d)/LanL2DZ level with Gaussian 09W.

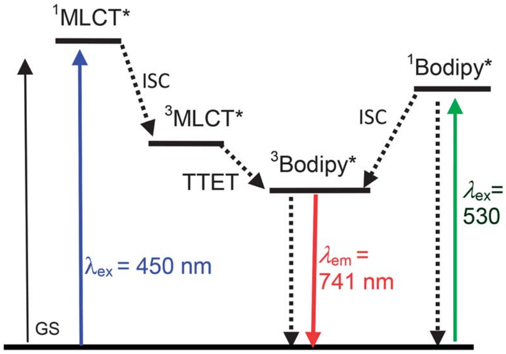

Scheme 2 Jablonski diagram of the photophysical processes involved in the photoexcitation and emission of **Ru-1**.

We studied the difference of the ground state geometry and the triplet state geometry, and found out that the geometry changes occurred at the Bodipy π-conjugated core. The Ru(II) coordination framework and the ethynyl linker did not show any substantial geometrical changes. This observation is in full agreement with the transient absorption studies, as well as the DFT calculation. That is, the triplet states of **Ru-1** and **Ru-2** are localized on the Bodipy moiety.

Based on the absorption and emission of the ligands and the complexes, the photophysical processes involved in **Ru-1** can be summarized in Scheme 2.[25,46,58] For **Ru-1**, the direct ^{1}Bodipy* → ^{3}Bodipy* ISC is efficient, therefore the residual fluorescence of Bodipy is very weak. The ^{3}MLCT* phosphorescence was also quenched due to the ^{3}MLCT* → ^{3}Bodipy* energy transfer. For **Ru-2**, the ^{1}Bodipy* → ^{3}Bodipy* ISC is non-efficient, therefore the residual fluorescence of the Bodipy ligand is more significant. Based on the excitation spectrum, we propose that the ^{1}MLCT* → ^{1}Bodipy* energy transfer is non-efficient, due to the fast ^{1}MLCT* → ^{3}MLCT* ISC, therefore excitation into the MLCT band of **Ru-2** cannot produce the fluorescence of the Bodipy ligand. Excitation into the Bodipy cannot produce the ^{3}MLCT state efficiently, indicating that the CS state has a lower energy level than the ^{3}MLCT state.[25]

Application of the complexes in triplet–triplet annihilation upconversion

Bodipy-containing Ru(II) complexes have never been used for any photophysical processes.[25,46] The new complexes we prepared show strong absorption of visible light and exceptionally long-lived triplet excited states, which are suitable to be used as triplet photosensitizers. Therefore these complexes were used for TTA upconversion (Fig. 8). With excitation at 532 nm, weak luminescence was observed for the complexes (Fig. 8a). With addition of the triplet acceptor perylene, strong blue emission was observed with **Ru-1** as the triplet photosensitizer (Fig. 8b). Excitation of **Ru-1** or perylene alone at 532 nm did not produce this emission band, thus the TTA upconversion was proved. For **Ru-2** and **Ru-3**, however, no upconversion was observed. Another reference complex Ru(dmb)$_3$[PF$_6$]$_2$ was also

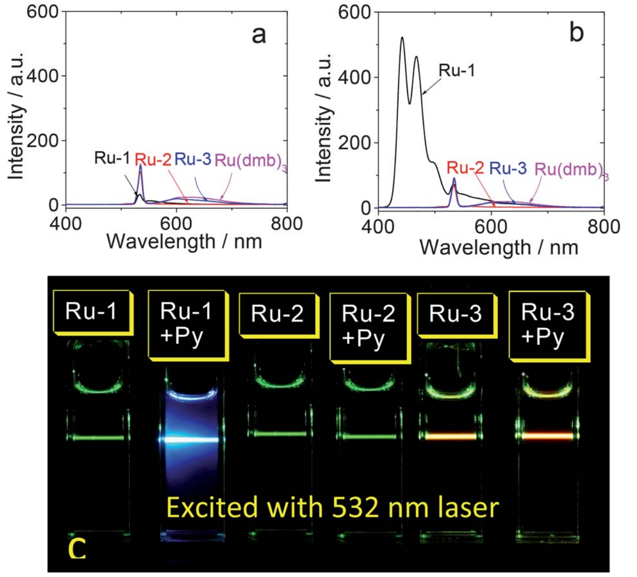

Fig. 8 Upconversion with **Ru-1**, **Ru-2**, **Ru-3** and Ru(dmb)$_3$[PF$_6$]$_2$ as triplet sensitizers (1.0 × 10^{-5} M). (a) Emission spectra without perylene and (b) emission spectra with perylene added. (c) Photographs of the emission of sensitizers alone and in the presence of perylene (Py) (4.1 × 10^{-5} M). Excited with green laser, λ_{ex} = 532 nm, 11.2 mW (MeCN, 20 °C).

studied but no upconversion was observed under the experimental conditions.

The upconversion is clearly visible to unaided eye (Fig. 8c). Without the triplet acceptor perylene, the colour of the laser beam is green, due to the very weak emission of the complex **Ru-1** and the scattered 532 nm laser. In the presence of the triplet acceptor perylene, strong blue emission was observed. To the best of our knowledge, this is the first time that the green light-excitable Ru(II) complex was used for TTA upconversion.[62,63] Previously Ru(dmb)$_3$[PF$_6$]$_2$ (dmb = 4,4′-dimethyl-2,2′-bipyridine), and Ru(II) complexes with long-lived triplet excited states were used for TTA upconversion, but all these Ru(II) complexes show absorption maxima in the blue region.[53,54,64–66] One Ru(II) containing triplet photosensitizer was reported to be near IR-excitable for TTA upconversion, but the light-harvested chromophore is not the Ru(II) coordination moiety.[67]

Since the ligand fluorescence is almost completely quenched in **Ru-2**, and the nanosecond time-resolved transient difference absorption spectra confirmed the population of the triplet excited states of **Ru-2**, we propose that TTA upconversion can be observed with appropriate excitation wavelength. Furthermore, in order to directly compare the TTA upconversion efficiency with **Ru-1** and **Ru-2** as the triplet photosensitizer, the TTA upconversion with **Ru-1** and **Ru-2** as the photosensitizers at the same excitation wavelength was carried out (Fig. 9). The results show that the TTA upconversion with **Ru-1** is *ca.* 2-fold to that with **Ru-2** as the triplet photosensitizer. This result indicates that the generation of the triplet excited state in **Ru-1** is more efficient than that in **Ru-2**. Note that both **Ru-1** and **Ru-2** show the same absorbance at the excitation wavelength.

In order to study the efficiency of the TTET process, the quenching of the triplet state lifetime of the Ru(II) complexes in the presence of triplet acceptor perylene was studied and the Stern–Volmer quenching curves were plotted (Fig. 10). We found that the quenching of the triplet excited state of **Ru-1** and **Ru-2** by perylene is significant. For **Ru-3**, however, the quenching effect is neglectable. These different quenching efficiencies are due to the different triplet excited state lifetimes of **Ru-1** and **Ru-2**. The quenching constants of **Ru-1** and **Ru-2** are 650–790-fold of **Ru-3**. Therefore the long-lived triplet excited state of the triplet photosensitizers is beneficial for the TTA upconversion. The TTA upconversion quantum yield of **Ru-1** is *ca.* 2-fold of **Ru-2**. The overall upconversion capacity, with consideration of the absorption of the triplet photosensitizer at the photoexcitation wavelength, was also compared (Table 2).

In order to unambiguously prove that the blue emission is due to the TTA upconversion, the lifetime of the blue emission observed in the TTA upconversion experiments was studied (Fig. 11). For **Ru-1** and **Ru-2**, the lifetimes of the emission at 450 nm were determined as 162.0 μs and 180.9 μs, respectively. The lifetime of the prompt fluorescence of perylene was determined as 4.0 ns in a different experiment. Therefore, the exceptionally long-lived luminescence lifetime with **Ru-1**/perylene and **Ru-2**/pyrelene is attributed to the TTA upconversion.[68–74] The photophysical parameters related to the TTA upconversion are listed in Table 2.

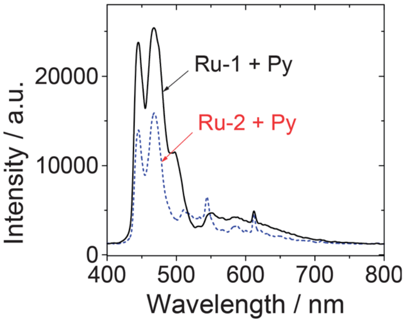

Fig. 9 Upconversion with **Ru-1** and **Ru-2** as the photosensitizers (1.0 × 10^{-5} M), perylene (Py) (4.1 × 10^{-5} M) as the acceptor, excited by the OPO laser at the isosbestic point of the UV/Vis absorption of **Ru-1** and **Ru-2** (509 nm) (deaerated MeCN, 20 °C).

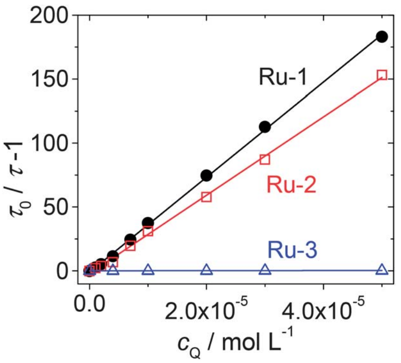

Fig. 10 Stern–Volmer plots generated from triplet excited state lifetime (τ_T) quenching of complexes **Ru-1**, **Ru-2** or phosphorescence intensity quenching of **Ru-3** measured as a function of perylene concentration in MeCN. The lifetimes were measured with the nanosecond time-resolved transient absorption. The concentration of the photosensitizers was fixed at 1.0 × 10^{-5} M, 20 °C.

Table 2 Triplet excited state lifetimes (τ_T), Stern–Volmer quenching constant (K_{SV}) and bimolecular quenching constants (k_q) of **Ru-1**, **Ru-2** and **Ru-3** as the photosensitizers. Perylene was used as the quencher. In deaerated MeCN solution, 20 °C

	τ_{DF}/μs	K_{sv}[a]	k_q[b]	Φ_{UC}[c]	η[d]
Ru-1	162.0	3718.5	13.3	1.2%	751.2
Ru-2	180.9	3065.5	12.4	0.7%	201.6
Ru-3	—[e]	4.7	5.9	—[e]	—[e]

[a] Quenching constants in 10^3 M^{-1}. [b] Bimolecular quenching constants in 10^9 M^{-1} s^{-1}. [c] Excited with a 532 nm laser, with the prompt fluorescence of iodo-BDP as the standard (Φ = 2.7% in MeCN). [d] Overall upconversion ability, $\eta = \varepsilon \times \Phi_{UC}$, in 10^3 M^{-1} cm^{-1}. [e] Too low to be determined accurately.

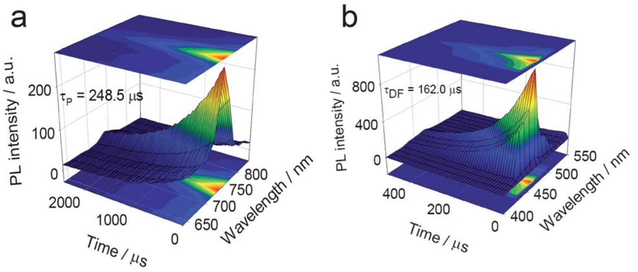

Fig. 11 Time-resolved emission spectra (TRES) of (a) the complex **Ru-1** and (b) the upconverted fluorescence of perylene using **Ru-1** as the triplet photosensitizers. Excited with the nanosecond pulsed OPO laser. **Ru-1**: $c = 1.0 \times 10^{-5}$ M. Py: $c = 4.1 \times 10^{-5}$ M. In deaerated MeCN, 20 °C.

The photophysical process involved in the TTA upconversion with the Ru(II) complexes as triplet photosensitizers can be summarized in Scheme 3. Excitation into both the MLCT and the IL bands of **Ru-1** will produce the ^{3}IL state, which is localized on Bodipy. The triplet–triplet-energy-transfer (TTET) between the Ru(II) complexes and the triplet acceptor perylene will produce the triplet excited state of the acceptor. TTA of the acceptor will produce the singlet excited state and the radiative decay of the singlet excited state will give the upconverted fluorescence from perylene (delayed fluorescence). The light-harvesting ability and the lifetime of the Ru(II) photosensitizer are crucial for TTA upconversion.

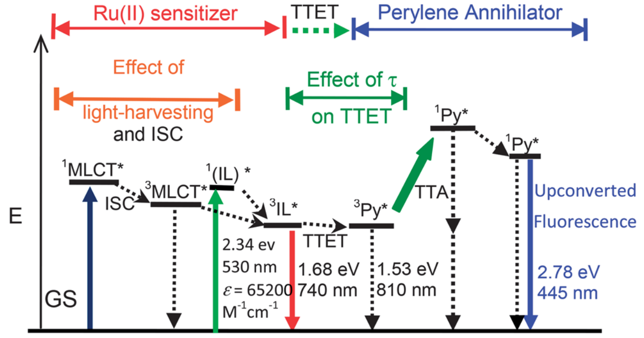

Scheme 3 Jablonski diagram of triplet–triplet-annihilation (TTA) upconversion with **Ru-1** as a triplet photosensitizer and perylene as a triplet acceptor. The effect of the light-harvesting ability and the triplet lifetimes of the Ru(II) sensitizers on the efficiency of the TTA-upconversion are also shown. *E* is the energy. GS is the ground state (S_0). ^{1}MLCT* is the Ru(II) based metal-to-ligand-charge-transfer singlet excited state, ^{1}IL* is the Bodipy localized intraligand singlet excited state. ^{3}MLCT* is the Ru(II) based metal-to-ligand-charge-transfer triplet excited state. ^{3}IL* is the Bodipy localized intraligand triplet excited state. TTET is the triplet–triplet energy transfer. ^{3}Py* is the triplet excited state of perylene. TTA is the triplet–triplet annihilation. ^{1}Py* is the singlet excited state of perylene. The emission bands observed in the TTA experiment are the singlet emission of perylene (delayed fluorescence).

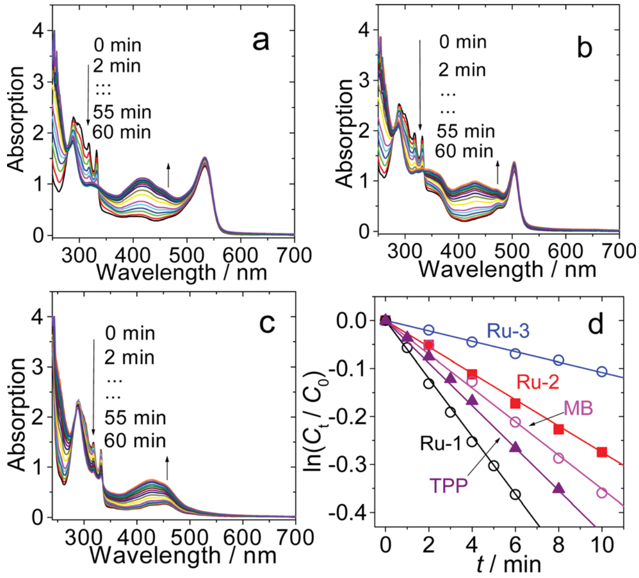

Fig. 12 UV-Vis absorption spectral change for DHN using (a) complex **Ru-1**, (b) **Ru-2**, (c) **Ru-3**, (d) plots of $\ln(C_t/C_0)$ *vs.* irradiation time (*t*) for the photo-oxidation of DHN using Ru complexes. Irradiated with a 35 W xenon lamp (13 mW cm^{-2} in the photoreactor; the UV light with a wavelength shorter than 385 nm was blocked by 0.72 M $NaNO_2$ solution). In CH_2Cl_2–CH_3OH (9 : 1, v/v); *c* [DHN] = 2.0×10^{-4} M; *c* [photosensitizer] = 2.0×10^{-5} M; 20 °C.

Photosensitization of singlet oxygen ($^1O_2$): photoxidation with the complexes as a triplet photosensitizer

These complexes were also used as a triplet photosensitizer for other photophysical process that involved TTET, herein we studied the singlet oxygen ($^1O_2$)-mediated photooxidation, with 1,5-dihydroxynaphthalene (DHN) as the $^1O_2$ scavenger to follow the kinetics of the $^1O_2$ production of the triplet

Table 3 Pseudo-first-order kinetics parameters, $^1O_2$ generation quantum efficiencies and yields of Juglone for the photo-oxidations of DHN using complexes **Ru-1–Ru-3** and MB, TPP as sensitizers

	τ_T/μs	k_{obs}/min^{-1}	ν_i[a]	Φ_Δ[b]	Yield[d] (%)
Ru-1	279.7	0.0603	1.206	0.93	96.5
Ru-2	246.6	0.0275	0.55	0.64	93.3
Ru-3	0.8	0.0108	0.216	0.66[c]	66.2
TPP	82.5	0.0443	0.886	0.65	96.9
MB	83.3	0.0351	0.702	0.57	83.7

[a] 10^{-5} M min^{-1}. Initial rate of DHN consumption. [b] $^1O_2$ generation quantum yield measured using Rose Bengal (Φ_Δ = 0.80 in MeOH) as a reference, λ_{ex} = 509 nm. [c] TPP (Φ_Δ = 0.65 in CH_2Cl_2) as a reference. λ_{ex} = 428 nm. [d] Yield of juglone after 60 min of photoreaction.

photosensitizers.[45,75–78] The photo-oxidation product juglone can be used for preparation of anti-cancer compounds.[79,80] The conventional triplet photosensitizers *meso*-tetraphenylporphyrin (TPP) and methylene blue (MB) were studied for comparison. The results show that the $^1O_2$ production of **Ru-1** is more efficient than **Ru-2**, which indicates that the ISC in **Ru-1** is more efficient than that in **Ru-2**. The $^1O_2$ production ability of **Ru-1** is more efficient than TPP and MB (Fig. 12). To the best of knowledge, very few triplet photosensitizers were reported to be more efficient than TPP and MB as $^1O_2$ photosensitizers.

The $^1O_2$ quantum yields of the triplet photosensitizers were determined (Table 3). Much higher Φ_Δ values were found for **Ru-1** (0.93) than **Ru-2** (0.64). These results indicated that the molecular structural profile of **Ru-1**, *i.e.* the π-conjugation between the coordination center and Bodipy is favorable for ISC.

Conclusion

In summary, we prepared two Bodipy-containing polyimine Ru(II) complexes. For **Ru-1**, the Bodipy and the coordination center are π-conjugated *via* a C≡C bond, which is a new molecular structural profile for Bodipy-containing Ru(II) complexes. For **Ru-2**, however, the π-core of the Bodipy chromophore and the coordination center are separated by a phenyl moiety, which is the known structural profile for the Bodipy-containing Ru(II) complexes. $Ru(bpy)_3[PF_6]_2$ (**Ru-3**) was used as a reference complex. Both **Ru-1** and **Ru-2** show strong absorption in the visible region (ε is up to 65 200 M^{-1} cm^{-1} at 528 nm), which is in stark contrast to **Ru-3**, which show the typical weak absorption in the visible region of the normal Ru(II) polyimine complexes ($\varepsilon = 11\,400$ M^{-1} cm^{-1} at 451 nm). The ligand fluorescence was substantially quenched in both **Ru-1** and **Ru-2**. RT near IR emission of the Bodipy part was observed with **Ru-1**, but not with **Ru-2**. This is the first time that the RT near IR phosphorescence of Bodipy was observed in Ru(II) complexes. Bodipy-localized long-lived triplet excited states were populated for **Ru-1** and **Ru-2** (τ_T is up to 279.7 μs), based on the nanosecond transient absorption spectrum, and was supported by the spin density analysis. To the best of our knowledge, this is the longest triplet excited state lifetime observed for the Bodipy chromophore. The complexes were used as triplet photosensitizers for two triplet–triplet-energy-transfer (TTET)-related processes, *i.e.* triplet–triplet annihilation upconversion and singlet oxygen ($^1O_2$) mediated photo-oxidation. In both applications **Ru-1** demonstrated higher efficiency (singlet oxygen quantum yield $\Phi_\Delta = 0.93$) than that of **Ru-2** ($\Phi_\Delta = 0.64$). These results indicated that the π-conjugation between the Bodipy chromophore and the Ru(II) coordination center is essential for enhancement of the effective visible light absorption of the Ru(II) complexes, *i.e.* efficient energy funneling from the Bodipy part to the triplet state manifold can be resulted. In contrast, the known method of tethering a chromophore on the complex (without any π-conjugation between the visible light-harvesting organic chromophore and the Ru(II) coordination center) is less efficient to produce effective visible light absorption for the Ru(II) complexes. These results are useful for designing of Ru(II) complexes that show strong absorption of visible light and long-lived triplet excited state and for the application of these complexes in the area of photocatalysis, photodynamic therapy and triplet–triplet-annihilation upconversion.

Acknowledgements

We thank the NSFC (20972024, 21073028 and 21273028), the Royal Society (UK) and NSFC (China-UK Cost-Share Science Networks, 21011130154), Science Foundation Ireland (SFI E.T.S. Walton Program 11/W.1/E2061) and Ministry of Education (NCET-08-0077 and SRFDP-20120041130005) for financial support.

Notes and references

1 (*a*) E. Baranoff, J.-P. Collin, L. Flamigni and J.-P. Sauvage, *Chem. Soc. Rev.*, 2004, **33**, 147–155; (*b*) J. Xuan and W.-J. Xiao, *Angew. Chem., Int. Ed.*, 2012, **51**, 6828–6838; (*c*) L. Shi and W. Xia, *Chem. Soc. Rev.*, 2012, **41**, 7687–7697.

2 (*a*) S. Campagna, F. Puntoriero, F. Nastasi, G. Bergamini and V. Balzani, *Top. Curr. Chem.*, 2007, **280**, 117–214; (*b*) A. Barbieri, B. Ventura and R. Ziessel, *Coord. Chem. Rev.*, 2012, **256**, 1732–1741.

3 (*a*) Q.-X. Zhou, W.-H. Lei, Y. Sun, J.-R. Chen, C. Li, Y.-J. Hou, X.-S. Wang and B.-W. Zhang, *Inorg. Chem.*, 2010, **49**, 4729–4731; (*b*) G. J. Ryan, S. Quinn and T. Gunnlaugsson, *Inorg. Chem.*, 2008, **47**, 401–403; (*c*) J. Lalevée, M. Peter, F. Dumur, D. Gigmes, N. Blanchard, M.-A. Tehfe, F. Morlet-Savary and J. P. Fouassier, *Chem.–Eur. J.*, 2011, **17**, 15027–15031; (*d*) M. Rueping, R. M. Koenigs, K. Poscharny, D. C. Fabry, D. Leonori and C. Vila, *Chem.–Eur. J.*, 2012, **18**, 5170–5174.

4 (*a*) F. Lakadamyaliy and E. Reisne, *Chem. Commun.*, 2011, **47**, 1695–1697; (*b*) F. Gärtner, D. Cozzula, S. Losse, A. Boddien, G. Anilkumar, H. Junge, T. Schulz, N. Marquet, A. Spannenberg, S. Gladiali and M. Beller, *Chem.–Eur. J.*, 2011, **17**, 6998–7006; (*c*) W.-G. Wang, F. Wang, H.-Y. Wang, C.-H. Tung and L.-Z. Wu, *Dalton Trans.*, 2012, **41**, 2420–2426.

5 B. Armitage, *Chem. Rev.*, 1998, **98**, 1171–1200.

6 H. J. Bolink, E. Coronado, R. D. Costa, P. Gaviña, E. Ortí and S. Tatay, *Inorg. Chem.*, 2009, **48**, 3907–3909.

7 R. Zhang, Z. Ye, G. Wang, W. Zhang and J. Yuan, *Chem.–Eur. J.*, 2010, **16**, 6884–6891.

8 (*a*) Q. Zhao, F. Li and C. Huang, *Chem. Soc. Rev.*, 2010, **39**, 3007–3030; (*b*) V. Fernández-Moreira, F. L. Thorp-Greenwood and M. P. Coogan, *Chem. Commun.*, 2010, **46**, 186–202; (*c*) T. A. Miller, J. C. Jeffery, M. D. Ward, H. Adams, S. J. A. Pope and S. Faulkner, *Dalton Trans.*, 2004, 1524–2152.

9 R. B. P. Elmes, M. Erby, S. A. Bright, D. C. Williams and T. Gunnlaugsson, *Chem. Commun.*, 2012, **48**, 2588–2590.

10 Y. Sun, Z. M. Hudson, Y. Rao and S. Wang, *Inorg. Chem.*, 2011, **50**, 3373–3378.

11 (*a*) R. B. P. Elmes, K. N. Orange, S. M. Cloonan, D. C. Williams and T. Gunnlaugsson, *J. Am. Chem. Soc.*, 2011, **133**, 15862–15865; (*b*) C. Wang and W. Lin, *J. Am. Chem. Soc.*, 2011, **133**, 4232–4235.

12 (*a*) Y. Chi and P.-T. Chou, *Chem. Soc. Rev.*, 2010, **39**, 638–655; (*b*) O. S. Wenger, *Chem.–Eur. J.*, 2011, **17**, 11692–11702; (*c*) S. Diring, R. Ziessel, F. Barigelletti, A. Barbieri and B. Ventura, *Chem.–Eur. J.*, 2010, **16**, 9226–9236; (*d*) Q.-X. Zhou, W.-H. Lei, J.-R. Chen, C. Li, Y.-J. Hou, X.-S. Wang and B.-W. Zhang, *Chem.–Eur. J.*, 2010, **16**, 3157–3165; (*e*) C.-Y. Wong, G. S. M. Tong, C.-M. Che and N. Zhu, *Angew. Chem., Int. Ed.*, 2006, **45**, 2694–2698; (*f*) S. P. Foxon, M. A. H. Alamiry, M. G. Walker, A. J. H. M. Meijer, I. V. Sazanovich, J. A. Weinstein and J. A. Thomas, *J. Phys. Chem. A*, 2009, **113**, 12754–12762; (*g*) J. A. Gareth Williams, *Top. Curr. Chem.*, 2007, **281**, 205–268.

13 (*a*) V. Friese, S. Nag, J. Wang, M.-P. Santoni, A. Rodrigue-Witchel, G. S. Hanan and F. Schaper, *Eur. J. Inorg. Chem.*, 2011, 39–44; (*b*) W.-Y. Wong and C.-L. Ho, *Coord. Chem. Rev.*, 2009, **253**, 1709–1758.

14 C.-J. Yao, R.-H. Zheng, Q. Shi, Y.-W. Zhong and J. Yao, *Chem. Commun.*, 2012, **48**, 5680–5682.

15 M. B. Majewski, N. R. de Tacconi, F. M. MacDonnell and M. O. Wolf, *Inorg. Chem.*, 2011, **50**, 9939–9941.

16 (*a*) G. Li, L. Ray, E. N. Glass, K. Kovnir, A. Khoroshutin, S. I. Gorelsky and M. Shatruk, *Inorg. Chem.*, 2012, **51**, 1614–1624; (*b*) M. Falkenström, O. Johansson and L. Hammarström, *Inorg. Chim. Acta*, 2007, **360**, 741–775.

17 (*a*) T. N. Singh-Rachford and F. N. Castellano, *Coord. Chem. Rev.*, 2010, **254**, 2560–2573; (*b*) A. Monguzzi, R. Tubino, S. Hoseinkhani, M. Campione and F. Meinardi, *Phys. Chem. Chem. Phys.*, 2012, **14**, 4322–4332; (*c*) J. Sun, F. Zhong, X. Yi and J. Zhao, *Inorg. Chem.*, 2013, **52**, 6299–6310; (*d*) H.-C. Chen, C.-Y. Hung, K.-H. Wang, H.-L. Chen, W. S. Fann, F.-C. Chien, P. Chen, T. J. Chow, C.-P. Hsu and S.-S. Sun, *Chem. Commun.*, 2009, 4064–4066.

18 A. Harriman, M. Hissler, A. Khatyr and R. Ziessel, *Chem. Commun.*, 1999, 735–736.

19 K. Kalyanasundaram, *Coord. Chem. Rev.*, 1982, **46**, 159–244.

20 N. Armaroli, *ChemPhysChem*, 2008, **9**, 371–373.

21 N. D. McClenaghan, Y. Leydet, B. Maubert, M. T. Indelli and S. Campagna, *Coord. Chem. Rev.*, 2005, **249**, 1336–1350.

22 A. I. Baba, J. R. Shaw, J. A. Simon, R. P. Thummel and R. H. Schmehl, *Coord. Chem. Rev.*, 1998, **171**, 43–59.

23 E. A. Medlycott and G. S. Hanan, *Chem. Soc. Rev.*, 2005, **34**, 133–142.

24 D. S. Tyson, J. Bialecki and F. N. Castellano, *Chem. Commun.*, 2000, 2355–2356.

25 M. Galletta, S. Campagna, M. Quesad, G. Ulrich and R. Ziessel, *Chem. Commun.*, 2005, 4222–4224.

26 E. A. Medlycott and G. S. Hanan, *Coord. Chem. Rev.*, 2006, **250**, 1763–1782.

27 D. S. Tyson, C. R. Luman, X. Zhou and F. N. Castellano, *Inorg. Chem.*, 2001, **40**, 4063–4071.

28 S. Ji, W. Wu, W. Wu, P. Song, K. Han, Z. Wang, S. Liu, H. Guo and J. Zhao, *J. Mater. Chem.*, 2010, **20**, 1953–1963.

29 S. Verma, P. Kar, A. Das and H. N. Ghosh, *Dalton Trans.*, 2011, **40**, 9765–9773.

30 Y. Liu, A. De Nicola, O. Reiff, R. Ziessel and K. S. Schanze, *J. Phys. Chem. A*, 2003, **107**, 3476–3485.

31 M. Abrahamsson, M. Jäger, T. Österman, L. Eriksson, P. Persson, H.-C. Becker, O. Johansson and L. Hammarström, *J. Am. Chem. Soc.*, 2006, **128**, 12616–12617.

32 D. S. Tyson and F. N. Castellano, *Inorg. Chem.*, 1999, **38**, 4382–4383.

33 X. Zhou, D. S. Tyson and F. N. Castellano, *Angew. Chem., Int. Ed.*, 2000, **39**, 4301–4305.

34 S. J. Smalley, M. R. Waterland and S. G. Telfer, *Inorg. Chem.*, 2009, **48**, 13–15.

35 G. Ulrich, R. Ziessel and A. Harriman, *Angew. Chem., Int. Ed.*, 2008, **47**, 1184–1201.

36 A. Loudet and K. Burgess, *Chem. Rev.*, 2007, **107**, 4891–4932.

37 A. Gorman, J. Killoran, C. O'Shea, T. Kenna, W. M. Gallagher and D. F. O'Shea, *J. Am. Chem. Soc.*, 2004, **126**, 10619–10631.

38 (*a*) X. Zhang, Y. Xiao and X. Qian, *Org. Lett.*, 2008, **10**, 19–32; (*b*) X.-D. Jiang, J. Zhang, T. Furuyama and W. Zhao, *Org. Lett.*, 2012, **14**, 248–251; (*c*) Y. Chen, J. Zhao, H. Guo and L. Xie, *J. Org. Chem.*, 2012, **77**, 2192–2206; (*d*) Y. Chen, J. Zhao, L. Xie, H. Guo and Q. Li, *RSC Adv.*, 2012, **2**, 3942–3953; (*e*) H. Guo, Y. Jing, X. Yuan, S. Ji, J. Zhao, X. Li and Y. Kan, *Org. Biomol. Chem.*, 2011, **9**, 3844–3853.

39 D. Wang, J. Fan, X. Gao, B. Wang, S. Sun and X. Peng, *J. Org. Chem.*, 2009, **74**, 7675–7683.

40 H. Lu, S. Shimizu, J. Mack, Z. Shen and N. Kobayashi, *Chem.–Asian J.*, 2011, **6**, 1026–1037.

41 T. Cheng, T. Wang, W. Zhu, X. Chen, Y. Yang, Y. Xu and X. Qian, *Org. Lett.*, 2011, **13**, 3656–3659.

42 Z. Kostereli, T. Ozdemir, O. Buyukcakir and E. U. Akkaya, *Org. Lett.*, 2012, **14**, 3636–3639.

43 F. Puntoriero, F. Nastasi, S. Campagna, T. Bura and R. Ziessel, *Chem.–Eur. J.*, 2010, **16**, 8832–8845.

44 M. E. El-Khouly, A. N. Amin, M. E. Zandler, S. Fukuzumi and F. D'Souza, *Chem.–Eur. J.*, 2012, **18**, 5239–5247.

45 N. Adarsh, M. Shanmugasundaram, R. R. Avirah and D. Ramaiah, *Chem.–Eur. J.*, 2012, **18**, 12655–12662.

46 M. Galletta, F. Puntoriero, S. Campagna, C. Chiorboli, M. Quesada, S. Goeb and R. Ziessel, *J. Phys. Chem. A*, 2006, **110**, 4348–4358.

47 O. A. Bozdemir, S. Erbas-Cakmak, O. O. Ekiz, A. Dana and E. U. Akkaya, *Angew. Chem., Int. Ed.*, 2011, **50**, 10907–10912.

48 Y. Wu, X. Peng, B. Guo, J. Fan, Z. Zhang, J. Wang, A. Cui and Y. Gao, *Org. Biomol. Chem.*, 2005, **3**, 1387–1392.

49 X. Zhang, Y. Xiao and X. Qian, *Org. Lett.*, 2008, **10**, 29–32.

50 O. A. Bozdemir, M. D. Yilmaz, O. Buyukcakir, A. Siemiarczuk, M. Tutas and E. U. Akkaya, *New J. Chem.*, 2010, **34**, 151–155.

51 (*a*) A. C. Benniston and G. Copley, *Phys. Chem. Chem. Phys.*, 2009, **11**, 4124–4131; (*b*) P. Batat, G. Vives, R. Bofinger, R.-W. Chang, B. Kauffmann, R. Oda, G. Jonusauskas and N. D. McClenaghan, *Photochem. Photobiol. Sci.*, 2012, **11**, 1666–1674.

52 R. Ziessel and A. Harriman, *Chem. Commun.*, 2011, **47**, 611–631.

53 S. Ji, W. Wu, W. Wu, H. Guo and J. Zhao, *Angew. Chem., Int. Ed.*, 2011, **50**, 1626–1629.

54 W. Wu, S. Ji, W. Wu, J. Shao, H. Guo, T. D. James and J. Zhao, *Chem.–Eur. J.*, 2012, **18**, 4953–4964.

55 W. Wu, H. Guo, W. Wu, S. Ji and J. Zhao, *J. Org. Chem.*, 2011, **76**, 7056–7064.

56 M. J. Frisch, *et al.*, *Gaussian 09, Revision 01*, Gaussian Inc., Wallingford, CT, 2009.

57 N. Adarsh, R. R. Avirah and D. Ramaiah, *Org. Lett.*, 2010, **12**, 5720–5723.

58 A. A. Rachford, R. Ziessel, T. Bura, P. Retailleau and F. N. Castellano, *Inorg. Chem.*, 2010, **49**, 3730–3736.

59 F. Nastasi, F. Puntoriero, S. Campagna, S. Diring and R. Ziessel, *Phys. Chem. Chem. Phys.*, 2008, **10**, 3982–3986.

60 E. Sakuda, Y. Ando, A. Ito and N. Kitamura, *Inorg. Chem.*, 2011, **50**, 1603–1613.

61 (*a*) C. I. Oprea, B. Frecuş, B. F. Minaev and M. A. Gîrţ, *Mol. Phys.*, 2011, **109**, 2511–2523; (*b*) B. F. Minaev, E. M. Khomenko and L. B. Yashchuk, *J. Appl. Spectrosc.*, 2009, **76**, 772–776; (*c*) S. Perumal, B. Minaev and H. Ågren, *J. Phys. Chem. C*, 2013, **117**, 3446–3455; (*d*) B. Minaev, V. Minaeva and H. Ågren, *J. Phys. Chem. A*, 2009, **113**, 726–735; (*e*) X. Li, B. Minaev, H. Ågren and H. Tian, *J. Phys. Chem. C*, 2011, **115**, 20724–20731; (*f*) X. Li, B. Minaev, H. Ågren and H. Tian, *Eur. J. Inorg. Chem.*, 2011, 2517–2524.

62 P. Ceroni, *Chem.–Eur. J.*, 2011, **17**, 9560–9564.

63 J. Zhao, S. Ji and H. Guo, *RSC Adv.*, 2011, **1**, 937–950.

64 R. R. Islangulov, D. V. Kozlov and F. N. Castellano, *Chem. Commun.*, 2005, 3776–3778.

65 S. Ji, H. Guo, W. Wu, W. Wu and J. Zhao, *Angew. Chem., Int. Ed.*, 2011, **50**, 8283–8286.

66 G. Bergamini, P. Ceroni, P. Fabbrizi and S. Cicchi, *Chem. Commun.*, 2011, **47**, 12780–12782.

67 T. N. Singh-Rachford, A. Nayak, M. L. Muro-Small, S. Goeb, M. J. Therien and F. N. Castellano, *J. Am. Chem. Soc.*, 2010, **132**, 14203–14211.

68 Y. Yap Cheng, T. Khoury, R. G. C. R. Clady, M. J. Y. Tayebjee, N. J. Ekins-Daukes, M. J. Crossley and T. W. Schmidt, *Phys. Chem. Chem. Phys.*, 2010, **12**, 66–71.

69 S. Guo, W. Wu, H. Guo and J. Zhao, *J. Org. Chem.*, 2012, **77**, 3933–3943.

70 S. Ji, W. Wu, J. Zhao, H. Guo and W. Wu, *Eur. J. Inorg. Chem.*, 2012, 3183–3190.

71 X. Yi, J. Zhao, W. Wu, D. Huang, S. Ji and J. Sun, *Dalton Trans.*, 2012, **41**, 8931–8940.

72 W. Wu, J. Zhao, J. Sun and S. Guo, *J. Org. Chem.*, 2012, **77**, 5305–5312.

73 H. Guo, Q. Li, L. Ma and J. Zhao, *J. Mater. Chem.*, 2012, **22**, 15757–15768.

74 S. Guo, J. Sun, L. Ma, W. You, P. Yang and J. Zhao, *Dyes Pigm.*, 2013, **96**, 449–458.

75 S.-Y. Takizawa, R. Aboshi and S. Murata, *Photochem. Photobiol. Sci.*, 2011, **10**, 895–903.

76 Y. Liu and J. Zhao, *Chem. Commun.*, 2012, **48**, 3751–3753.

77 J. Sun, J. Zhao, H. Guo and W. Wu, *Chem. Commun.*, 2012, **48**, 4169–4171.

78 L. Huang, X. Yu, W. Wu and J. Zhao, *Org. Lett.*, 2012, **14**, 2594–2597.

79 A. Thakur, *J. Med. Plants Res.*, 2011, **5**, 5324–5330.

80 P. Seshadri, A. Rajaram and R. Rajaram, *Free Radical Biol. Med.*, 2011, **51**, 2090–2107.